

SCIENTIFIC REPORTS



OPEN

Strong geologic methane emissions from discontinuous terrestrial permafrost in the Mackenzie Delta, Canada

Katrin Kohnert¹, Andrei Serafimovich¹, Stefan Metzger^{2,3}, Jörg Hartmann⁴ & Torsten Sachs¹

Arctic permafrost caps vast amounts of old, geologic methane (CH₄) in subsurface reservoirs. Thawing permafrost opens pathways for this CH₄ to migrate to the surface. However, the occurrence of geologic emissions and their contribution to the CH₄ budget in addition to recent, biogenic CH₄ is uncertain. Here we present a high-resolution (100 m × 100 m) regional (10,000 km²) CH₄ flux map of the Mackenzie Delta, Canada, based on airborne CH₄ flux data from July 2012 and 2013. We identify strong, likely geologic emissions solely where the permafrost is discontinuous. These peaks are 13 times larger than typical biogenic emissions. Whereas microbial CH₄ production largely depends on recent air and soil temperature, geologic CH₄ was produced over millions of years and can be released year-round provided open pathways exist. Therefore, even though they only occur on about 1% of the area, geologic hotspots contribute 17% to the annual CH₄ emission estimate of our study area. We suggest that this share may increase if ongoing permafrost thaw opens new pathways. We conclude that, due to permafrost thaw, hydrocarbon-rich areas, prevalent in the Arctic, may see increased emission of geologic CH₄ in the future, in addition to enhanced microbial CH₄ production.

The emission of biogenic methane (CH₄) from arctic permafrost landscapes caused by microbial decomposition of carbon is widely discussed^{1–6}. The carbon pool of arctic permafrost soils is estimated at 1300 Pg (ref. 7). Emission estimates of biogenic CH₄ from permafrost regions vary between 32 and 112 Tg per year⁸. The production of biogenic CH₄ in wetlands is limited to soil temperatures allowing for microbial activity. This is the case during the warm season of the year, but also at soil temperatures around 0 °C, the “zero curtain”⁹.

In addition to the biogenic CH₄ sources, oil and gas reservoirs in the Arctic contain vast amounts of old, geologic CH₄ (ref. 10) that can be of biogenic or thermogenic origin. Currently, in large areas this source is sealed by a cap of permafrost. Geologic CH₄ can reach the surface if pathways in this cap exist along faults (cf. ref. 11 for lower latitudes) or form due to permafrost thawing^{12,13}. For subsea permafrost no consensus has been reached on the amount of geologic CH₄ released from e.g. the Siberian shelf^{14,15}. In terrestrial permafrost landscapes geologic CH₄ can reach the surface through open taliks (=thaw bulbs) below lakes¹³, or in the unfrozen areas of discontinuous permafrost, comparable to what was shown for lower latitudes^{11,16}. Until now, the occurrence of the entirety of these geologic sources in the Arctic and their contribution to the overall CH₄ emission is uncertain.

Among the largest amounts of oil and natural gas in the Arctic are likely stored in the Canadian Mackenzie Delta and its surroundings¹⁰. In this region, strong natural gas seeps have been described sporadically^{17,18}, some of which are fed by thermogenic CH₄ (refs 17–19). The permafrost in the delta is of the non-Yedoma type, i.e. without the ice-rich, organic rich characteristics of Yedoma permafrost²⁰. The permafrost state in our study area shows differences due to glaciation history and surface characteristics²¹. The delta itself is characterized by relatively thin (i.e. up to 100 m) and discontinuous permafrost as it was glaciated during the Pleistocene and waterbodies and channels are changing the surface and warming the ground²¹. The region east of the delta was unglaciated during the Pleistocene²² resulting in a sharp increase in permafrost thickness between the delta and

¹GFZ German Research Centre for Geosciences, Telegrafenberg, 14473 Potsdam, Germany. ²National Ecological Observatory Network, Battelle, 1685 38th Street, Boulder, CO 80301, USA. ³University of Wisconsin-Madison, Dept. of Atmospheric and Oceanic Sciences, 1225 West Dayton Street, Madison, WI 53706, USA. ⁴Alfred Wegener Institute Helmholtz Centre for Polar and Marine Research (AWI), Am Handelshafen 12, 27570 Bremerhaven, Germany. Correspondence and requests for materials should be addressed to K.K. (email: katrin.kohnert@gfz-potsdam.de)

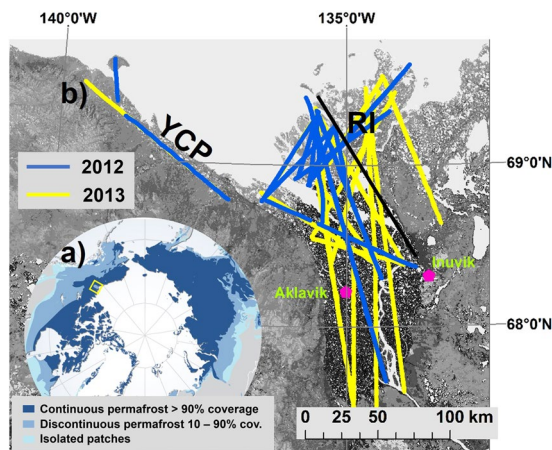


Figure 1. Study area and flight tracks. (a) Location of the study area and state of the permafrost (map modified after ref. 45), (b) flight tracks of two flight campaigns in 2012 and 2013 across the Mackenzie Delta, the adjacent Richards Island (RI) and the Yukon coastal plain (YCP). The black line marks the sharp transition between discontinuous permafrost in the delta to continuous permafrost on RI. The locations of the towns of Aklavik and Inuvik are shown for orientation. Data for background map from ref. 46. The map in Fig. 1b was created using ArcGIS software ArcMap 10.1 by Esri.

Richards Island (marked with black line in Fig. 1b). On Richards Island the permafrost is up to more than 500 m thick and continuous²¹ (Fig. 1b). On the Yukon coastal plain the permafrost thickness reaches about 300 m. The soil organic carbon stocks in the study area are classified as medium to high soil carbon content with mainly 50–70 kg m⁻² in the upper 1 m (ref. 7).

The overall aim of this study is to improve our understanding of geologic CH₄ emissions on a regional scale in the Mackenzie Delta region, Canada (Fig. 1). Therefore, the purpose of this study is twofold: (i) to map the CH₄ flux and its spatial variability at high spatial resolution and to derive the abundance of geologic CH₄ emission hotspots and (ii) to assess the relative contribution of biogenic and geologic sources to the annual CH₄ budget of the Mackenzie Delta region.

Results and Discussion

We conducted airborne eddy-covariance (EC) measurements (cf. ref. 23) covering large areas of the Mackenzie Delta region during two extensive campaigns in July 2012 and 2013 (Fig. 1b).

The CH₄ flux map (cf. ref. 24) resulting from our measurements covers 10,000 km² at a spatial resolution of 100 m × 100 m (Fig. 2a). This CH₄ flux map enables to detect spatial patterns in CH₄ emission and to identify and localize CH₄ emission hotspots in our entire study area. The median of all 2012 and 2013 CH₄ flux data was 1.1 mg m⁻² h⁻¹, which corresponds to fluxes measured by the EC technique in similar ecosystems^{25–29}. Most importantly, we found the largest emissions to be spatially stationary and temporally constant to <30% standard error, both within and between the two campaigns. A majority of high fluxes up to 14.7 mg CH₄ m⁻² h⁻¹ (with a standard error of <30%) occurred as clustered peaks in the northern part of the study area and only inside the delta (Fig. 2) where the permafrost is thin and discontinuous. Biogenic CH₄ emissions from arctic wetlands^{25–29} and lakes³⁰ are typically lower and driven by changing meteorological and surface properties, making stationary, repeatedly observable emission peaks at this strength and spatial extent unlikely.

For lack of isotopic data, we used published biogenic CH₄ flux data from EC flux tower measurements in the Arctic north of 61 °N for a conservative, approximate separation between biogenic emissions and strong geologic CH₄ hotspots. The area of influence of tower based EC measurements, the so-called footprint, is of a comparable spatial scale as those of our airborne EC measurements, integrating over several hectares. Measurements with chambers and bubble traps, on the other hand, cover much smaller scales and do not readily compare with spatially integrated EC measurements. They were therefore not considered for the following threshold definition. The maximum daily biogenic CH₄ flux from permafrost landscapes found in the literature is roughly 5.0 mg m⁻² h⁻¹ (e.g. refs 25–29; max. 4.58 mg m⁻² h⁻¹, ref. 28). At thermokarst margins of lakes with strong biogenic point sources, CH₄ emission can reach 5.0 mg m⁻² h⁻¹ as well¹³. Individual hotspots of biogenic CH₄ emission in lakes in carbon rich Yedoma type permafrost areas, can exceed that threshold³¹, but have an area of a few square metres, and thus are much smaller than the areas with CH₄ emission peaks that we observed. These high emissions from lakes do occur on a seep scale and their signal would disappear among neighbouring areas with less CH₄ emission, when we consider spatially integrated fluxes resulting from the EC method.

Therefore, we defined a flux of 5.0 mg m⁻² h⁻¹ as upper threshold for biogenic CH₄ fluxes from arctic permafrost landscapes. We thus assumed that reoccurring emissions exceeding 5 mg m⁻² h⁻¹ independently of atmospheric or surface conditions, day, time or year of flight, as found in the northern Mackenzie Delta, were not of recent biogenic origin. Instead, we attributed them to deeper geologic sources that release CH₄ through seeps, which can be related to taliks, faults or artificial pathways such as oil and gas exploration wells (Fig. 2).

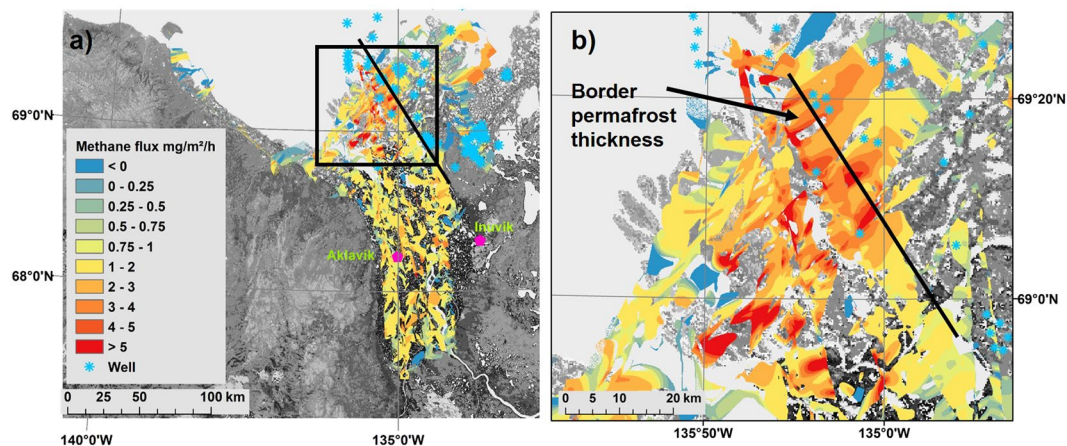


Figure 2. CH_4 flux map with location of wells. (a) CH_4 flux topography for both years containing data with a standard error $< 30\%$. Fluxes $> 5.0 \text{ mg m}^{-2} \text{ h}^{-1}$ are considered to be of geologic origin. Blue asterisks show the location of wells (oil or gas wells) derived from literature data. The locations of the towns of Inuvik and Aklavik are shown for orientation. (b) Magnification of the area with the highest CH_4 fluxes marked with the black square in Fig. 2a. Legend as in Fig. 2a. West of the black line the permafrost is discontinuous and thin, east of it continuous and thick. Data for background map from ref. 46. The map in Fig. 2 was created using ArcGIS software ArcMap 10.1 by Esri. Methods for deriving the CH_4 flux map are explained in chapters 4.2–4.5.

Combined, the footprints of our 2012 and 2013 measurements comprise $9,754 \text{ km}^2$ excluding areas with a standard error $> 30\%$. We find that about 1% of the mapped area (116 km^2), releases CH_4 at rates exceeding $5 \text{ mg m}^{-2} \text{ h}^{-1}$. Single areas with these peak emissions are up to several square kilometres large. At this spatial extent, biogenic emissions from thermokarst lakes that exceeded this threshold have not been reported³⁰. Single biogenic seeps in lakes would not result in an integrated signal that large.

We only found areas with high emissions within the northern part of the delta where the permafrost thickness is less than 100 m and the permafrost is discontinuous²¹ and therefore permeable for gas from the subsurface. In contrast, on the adjacent coastal plain and Richards Island, with their continuous and thick permafrost of up to 300 m and more than 500 m, respectively, such high emissions were not observed. We attribute that absence of emission peaks, despite established natural gas and oil deposits in the region (Fig. 2), to the thick impermeable permafrost in these areas. These CH_4 reserves might eventually be emitted into the atmosphere if the permafrost cap becomes permeable due to thawing.

To estimate the contribution of geologic sources to the annual CH_4 emissions of the study region, we divided the year roughly into a season with and without biogenic emission. For the following calculations, we did not account for potential biogenic emission from hotspots along thermokarst lake margins during winter time^{6, 32, 33}, as they are weaker than geologic hotspots as described above. Biogenic emissions into the atmosphere from permafrost wetlands and lakes are largely limited to the growing or ice-free season, respectively, and the “zero curtain” period with soil temperatures near 0°C (cf. ref. 9). Once soil temperatures drop permanently further during the cold season, the CH_4 emissions decrease rapidly to close to $0 \text{ mg m}^{-2} \text{ h}^{-1}$ (ref. 9). We derived the period of potential biogenic CH_4 emissions from soil temperatures in 10 cm depth from the North American Regional Reanalysis data³⁴. In the particularly warm year of 2013, soil temperatures in the Mackenzie Delta exceeded -2°C on about 165 days from end of May to beginning of November. We used this duration for biogenic emissions in the following back-of-the-envelope calculations. In contrast, we assumed that the emission of CH_4 from strong geologic sources is constant throughout the year, as it is independent of recent microbial activity and causes sufficiently strong ebullition in water bodies to maintain pathways through the ice during winter¹³. Using the median fluxes of biogenic ($0.84 \text{ mg m}^{-2} \text{ h}^{-1}$) and geologic ($6.3 \text{ mg m}^{-2} \text{ h}^{-1}$) emissions, respectively, geologic CH_4 contributes 3 Gg to the overall 35 Gg CH_4 emitted within the covered area during the 165 days warm period. Annually, 38 Gg CH_4 are emitted within this area, including 6.4 Gg CH_4 from geologic sources. The geologic estimates are very conservative, first, because, fluxes $< 5 \text{ mg m}^{-2} \text{ h}^{-1}$ may also include a significant amount of CH_4 from weaker geologic sources and, secondly, because extrapolating July biogenic fluxes, which are at or near a possible seasonal peak, into the shoulder seasons might overestimate the contribution of biogenic sources. Relative to their areal coverage, strong geologic sources that occur in 1% of the area thus contribute a disproportionately large fraction of at least 17% of the emissions to the estimated annual budget, making geologic sources 20 times stronger CH_4 emitters than biogenic sources.

Conclusions

Our study suggests, first, that thinning permafrost in a warmer climate may not only result in the frequently reported and discussed increased emission of biogenic CH_4 , but also in increased emissions of geologic CH_4 , that is currently still trapped under thick, continuous permafrost, as new emission pathways open due to thawing permafrost.

Secondly, in other arctic regions with natural gas and oil reservoirs that are currently capped under mainly continuous permafrost, e.g. the North Slope of Alaska or Siberia¹⁰, CH₄ contributions from those geologic sources might need to be included when addressing future CH₄ emissions under ongoing permafrost thaw.

Thirdly, our results indicate that geologic CH₄ emissions may contribute strongly to the permafrost-carbon-climate feedback, especially in permafrost areas vulnerable to thawing and therefore warrant much more attention.

Methods

Experimental Setup. This study was performed in the Mackenzie Delta, which is the second largest arctic delta (13,000 km²), along the adjacent Yukon coastal plain towards Herschel Island, and on Richards Island to the north east of the delta (67°26'N–69°33'N, 133°22'W–140°5'W). The study area extended about 320 km from west to east and had a north-south extension of 240 km. The study period was from July 4th to July 10th, 2012 (5 flight days, 44 flight tracks) and July 19th to July 26th, 2013 (7 flight days, 40 flight tracks).

Measurements were conducted aboard the research aircraft Polar 5 of the Alfred Wegener Institute Helmholtz Centre for Polar and Marine Sciences (AWI). A 3 m nose boom including a 5-hole probe for measuring the 3D wind vector was mounted to the front of the airplane. Sample air was drawn from an inlet above the cabin at about 9.71 s⁻¹ and analysed in an RMT-200 (Los Gatos Research Inc., Mountain View, California, USA) in 2012 (CH₄ concentration only) and a Fast Greenhouse Gas Analyser FGGA 24EP (Los Gatos Research Inc.) in 2013 (CH₄, carbon dioxide and water vapour). Gas concentrations were recorded at 20 Hz, wind speed at 100 Hz. Additionally, the aircraft was equipped with an Inertial Navigation System (Type Laser V, Honeywell International Inc., Morristown, New Jersey, USA), several Global Positioning Systems (NovAtel Inc., Calgary, Alberta, USA), a radar altimeter (KRA 405B/Honeywell International Inc., Morristown, New Jersey, USA) and a laser altimeter (LD90/RIEGL Laser Measurements Systems GmbH, Horn, Austria). Air temperature was measured with an open wire Pt100 in an unheated Rosemount housing, and air humidity with an HMT-330 (Vaisala, Helsinki, Finland) placed in a Rosemount housing. We derived the wind components *u*, *v*, and *w* with respect to the earth coordinate system using the method suggested by ref. 35. For the analysis only flux measurements derived after the warming up phase of the gas analysers (about 0.5 h) were used. Flight altitude was between 40–80 m above ground level, true airspeed was 60 ms⁻¹. A height dependency of CH₄ fluxes was not considered in our calculation. The atmospheric boundary layer (ABL) was determined with *in-situ* measurements of relative humidity and potential temperature during vertical profile flights at the beginning and end of each track. Flights above the ABL were excluded from the analysis.

Flux calculation. The data were analysed in GNU R version 2.15.3 using an early version of the eddy4R software³⁶. The analysis is based on 20 Hz dry mole fraction data. We calculated the dry mole fraction by using the humidity information from the Vaisala HMT-330 in 2012, and that from the FGGA itself for the 2013 data. Spectroscopic correction of the data was done following ref. 37. CH₄ fluxes were calculated with a time-frequency-resolved version of the eddy covariance technique using vertical wind speed and CH₄ concentration data²³. The result was an *in-situ* observed space-series of the surface-atmosphere exchange of CH₄ at 100 m spatial resolution. With a footprint model³⁸ the CH₄ emissions were related to the underlying surface. The data were quality controlled³⁹ and only data up to flag 6 (steady state and integral turbulence characteristics test ≤ 100%), the upper threshold for data that are considered eligible for long-term measurements, were included in the analysis. This left 66957 flux observations (=6696 km of flight tracks), more than 90% of the original data, as input data for our study. In this study we did not apply spectral, vertical flux divergence, and storage term corrections.

Flux topography calculation. To derive a flux map including CH₄ fluxes from all flights, we used the flux values along the flight tracks and the corresponding footprints. The footprints provide (i) the information about the location, size and shape of the area influencing the flux measurement at the respective point, and (ii) the percentage contribution, i.e. footprint weight, from each grid cell to the combined flux signal observed by the aircraft. The weight of the contribution of each grid cell depends mainly on the distance from the measurement point, wind direction, and atmospheric stratification. That is, the footprint itself does not separate the strengths of individual sources. Instead, for each grid cell this is achieved by superimposing joint replicates of footprint weights and corresponding flux observations as the aircraft passes by. In result, the flux gradient around strong emitters appears continuous rather than representing the potentially discrete nature of geologic features. This last discretization step is achieved by applying the >5 mg CH₄ m⁻² h⁻¹ thresholding.

We used flux topographies²⁴ to derive the CH₄ flux in each 100 m × 100 m grid cell using the sum of the products of CH₄ fluxes and footprint weights divided by the sum of footprint weights covering that grid cell

$$\frac{\sum_j^N \left(\sum_i^M f_{i,j} * g_{i,j} \right)}{\sum_j^N \left(\sum_i^M g_{i,j} \right)}$$

with the number of flight tracks *j* ... *N*, the number of footprint weights *i* ... *M* that cover a grid cell during a given flight track, the CH₄ flux *f* and the footprint weight *g*.

Error calculation. In this study error sources include random measurement error, error in the wavelet calculation and in the footprint calculation. Standard error topographies were calculated following ref. 40. Grid cells with a standard error <30% (963843 grid cells; 57% of the data) were included in the analysis. The shape of the CH₄ flux map presented in Fig. 2 is thus the result of the irregular shapes of the footprints caused by differences

in wind speed and direction, areas not included within the footprints of our CH₄ flux measurements, and the exclusion of these grid cells with a standard error >30%.

Anthropogenic features. In the ArcGIS software ArcMap 10.1 by Esri we digitalized, georeferenced and compiled information from the geologic maps of refs 41–44 and marked locations of exploration gas and oil wells in Fig. 2.

Estimating annual geologic and biogenic CH₄ emissions. The upper threshold for biogenic fluxes was set to 5 mg CH₄ m⁻² h⁻¹ based on maximum fluxes reported in the literature (e.g. refs 25–29). Emissions in grid cells exceeding this value were classified as geologic CH₄. We derived the period of potential biogenic CH₄ emissions from soil temperatures in 10 cm depth from the North American Regional Reanalysis (NARR) data³⁴. Microbial activity and CH₄ emission occurs in the warm period of the year and in the zero curtain period when soil temperatures fluctuate around 0 °C (ref. 9). CH₄ emissions decrease close to zero, once the soil temperature drops well below 0 °C for the duration of the cold season⁹. Therefore, we defined the period between spring and autumn with soil temperatures exceeding –2 °C as period with biogenic emissions. In our study region this period lasted for about 165 days from end of May to beginning of November. In contrast, strong geologic sources are assumed to release CH₄ to the surface continuously during 365 days a year if pathways exist. To calculate the emission from each of the two sources of CH₄, we used the respective time periods, area size of occurrence and the median fluxes. We used the median flux of all measurements equal to or larger than 5 mg m⁻² h⁻¹ (6.3 mg m⁻² h⁻¹) for geologic emissions, and the median of those emissions smaller 5 mg m⁻² h⁻¹ (0.84 mg m⁻² h⁻¹) for biogenic emissions.

References

1. Schuur, E. A. G. *et al.* Climate change and the permafrost carbon feedback. *Nature* **520**, 171–179 (2015).
2. Chang, R. Y.-W. *et al.* Methane emissions from Alaska in 2012 from CARVE airborne observations. *PNAS* **111**, 16694–16699 (2014).
3. Hodgkins, S. B. *et al.* Changes in peat chemistry associated with permafrost thaw increase greenhouse gas production. *PNAS* **111**, 5819–5824 (2014).
4. Melton, J. R. *et al.* Present state of global wetland extent and wetland methane modelling: conclusions from a model inter-comparison project (WETCHIMP). *Biogeosciences* **10**, 753–788 (2013).
5. Zona, D. *et al.* Methane fluxes during the initiation of a large-scale water table manipulation experiment in Alaskan Arctic tundra. *Glob. Biogeochem. Cycles* **23**, GB2013 (2009).
6. Walter, K. M., Zimov, S. A., Chanton, J. P., Verbyla, D. & Chapin, F. S. III Methane bubbling from Siberian thaw lakes as a positive feedback to climate warming. *Nature* **443**, 71–75 (2006).
7. Hugelius, G. *et al.* Estimated stocks of circumpolar permafrost carbon with quantified uncertainty ranges and identified data gaps. *Biogeosciences* **11**, 6573–6593 (2014).
8. McGuire, A. D. *et al.* Sensitivity of the carbon cycle in the Arctic to climate change. *Ecol. Monogr.* **79**, 523–555 (2009).
9. Zona, D. *et al.* Cold season emissions dominate the Arctic tundra methane budget. *PNAS* **113**, 40–4 (2016).
10. Gautier, D. L. *et al.* Assessment of Undiscovered Oil and Gas in the Arctic. *Science* **324**, 1175–1179 (2009).
11. Etiope, G. & Klusman, R. W. Microseepage in drylands: Flux and implications in the global atmospheric source/sink budget of methane. *Glob. Planet. Change* **72**, 265–274 (2010).
12. Romanovsky, V. E., Smith, S. L. & Christiansen, H. H. Permafrost Thermal State in the Polar Northern Hemisphere during the International Polar Year 2007–2009: a Synthesis. *Permafrost Periglacial Process* **21**, 106–116 (2010).
13. Walter Anthony, K. M., Anthony, P., Grosse, G. & Chanton, J. Geologic methane seeps along boundaries of Arctic permafrost thaw and melting glaciers. *Nat. Geosci.* **5**, 419–426 (2012).
14. Thornton, B. F., Geibel, M. C., Crill, P. M., Humborg, C. & Mörth, C.-M. Methane fluxes from the sea to the atmosphere across the Siberian shelf seas. *Geophys. Res. Lett.* **43**, 5869–5877 (2016).
15. Shakhova, N. *et al.* Extensive Methane Venting to the Atmosphere from Sediments of the east Siberian Arctic Shelf. *Science* **327**, 1246–1250 (2010).
16. Etiope, G. & Klusman, R. W. Geologic emissions of methane to the atmosphere. *Chemosphere* **49**, 777–789 (2002).
17. Bowen, R. G., Dallimore, S. R., Côte, M. M., Wright, J. F. & Lorenson, T. D. Geomorphology and gas release from pockmark features in the Mackenzie Delta, Northwest Territories, Canada. In Proceedings of Ninth International Conference on Permafrost pp. 171–176, eds Kane, D. L. & Hinkel, K. M. Fairbanks, Alaska, Institute of Northern Engineering (2008).
18. Osadetz, K. G. & Chen, Z. A re-evaluation of Beaufort Sea-Mackenzie Delta basin gas hydrate resource potential: petroleum system approaches to non-conventional gas resource appraisal and geologically-sourced methane flux. *B. Can. Petrol. Geol.* **58**, 56–71 (2010).
19. Collett, T. S. & Dallimore, S. R. Hydrocarbon gases associated with permafrost in the Mackenzie Delta, Northwest Territories, Canada. *Appl. Geochem.* **14**, 607–620 (1999).
20. Strauss, J. *et al.* The deep permafrost carbon pool of the Yedoma region in Siberia and Alaska. *Geophys. Res. Lett.* **40**, 6165–6170 (2013).
21. Burn, C. R. & Kokelj, S. V. The Environment and Permafrost of the Mackenzie Delta Area. *Permafrost Periglacial Process* **20**, 83–105 (2009).
22. Taylor, A. E., Dallimore, S. R. & Judge, A. S. Late Quaternary history of the Mackenzie – Beaufort region, Arctic Canada, from modelling of permafrost temperatures. 2. The Mackenzie Delta – Tuktoyaktuk Coastlands. *Can. J. Earth Sci.* **33**, 62–71 (1996).
23. Metzger, S. *et al.* Spatially explicit regionalization of airborne flux measurements using environmental response functions. *Biogeosciences* **10**, 2193–2217 (2013).
24. Mauder, M., Desjardins, R. L. & MacPherson, I. Creating Surface Flux Maps From Airborne Measurements: Application to the Mackenzie Area GEWEX Study MAGS 1999. *Boundary-Layer Meteorol* **129**, 431–450 (2008).
25. Sturtevant, C. S., Oechel, W. C., Zona, D., Kim, Y. & Emerson, C. E. Soil moisture control over autumn season methane flux, Arctic Coastal Plain of Alaska. *Biogeosciences* **9**, 1423–1440 (2012).
26. Sachs, T., Wille, C., Boike, J. & Kutzbach, L. Environmental controls on ecosystem-scale CH₄ emission from polygonal tundra in the Lena River Delta, Siberia. *J. Geophys. Res.* **113**, G00A03 (2008).
27. Wille, C., Kutzbach, L., Sachs, T., Wagner, D. & Pfeiffer, E.-M. Methane emission from Siberian arctic polygonal tundra: eddy covariance measurements and modeling. *Glob. Change Biol.* **14**, 1395–1408 (2008).
28. Friborg, T., Christensen, T. R., Hansen, B. U., Nordstroem, C. & Soegaard, H. Trace gas exchange in a high-arctic valley 2. Landscape CH₄ fluxes measured and modelled using eddy correlation data. *Glob. Biogeochem. Cycles* **14**, 715–723 (2000).
29. Fan, S. M. *et al.* Micrometeorological Measurements of CH₄ and CO₂ Exchange Between the Atmosphere and Subarctic Tundra. *J. Geophys. Res.* **97**, 16,627–16,643 (1992).

30. Wik, M., Varner, R. K., Walter Anthony, K., MacIntyre, S. & Bastviken, D. Climate-sensitive northern lakes and ponds area critical components of methane release. *Nat. Geosci.* **9**, 99–106 (2016).
31. Walter Anthony *et al.* Methane emissions proportional to permafrost carbon thawed in Arctic lakes since the 1950s. *Nat. Geosci.* **9**, 679–682 (2016).
32. Zimov, S. A. *et al.* North Siberian Lakes: A Methane Source Fueled by Pleistocene Carbon. *Science* **277**, 800–802 (1997).
33. Sepulveda-Jauregui, A., Walter Anthony, K. M., Martinez-Cruz, K., Greene, S. & Thalasso, F. Methane and carbon dioxide emissions from 40 lakes along a north-south latitudinal transect in Alaska. *Biogeosciences* **12**, 3197–3223 (2015).
34. Mesinger, F. *et al.* North American Regional Reanalysis. *Bull. Am. Meteorol. Soc.* **87**, 343–360 (2006).
35. Lenschow, D. H. *Probing the Atmospheric Boundary Layer*. American Meteorological Society, Boston, Massachusetts, pp. 269 (1986).
36. Metzger, S. *et al.* eddy4R: A community-extensible processing, analysis and modeling framework for eddy-covariance data based on R, Git, Docker and HDF5. *Geosci. Model Dev. Discuss.* (2017).
37. Tuzson, B. Field intercomparison of two optical analyzers for CH₄ eddy covariance flux measurements. *Atmos. Meas. Tech.* **3**, 1519–1531 (2010).
38. Kormann, R. & Meixner, F. X. An analytical footprint model for non-neutral stratification. *Boundary-Layer Meteorol.* **99**, 207–224 (2001).
39. Foken, T. *Micrometeorology*. Springer-Verlag, Berlin, Heidelberg, pp. 308, ISBN: 978-3-540-74665-2 (2008).
40. Gatz, D. F. & Smith, L. The standard error of a weighted mean concentration – I. Bootstrapping vs other methods. *Atmos. Environ.* **29**, 1185–1193 (1995).
41. Dallimore, S. & Collett, T. S. Scientific results from the Mallik 2002 gas hydrate production research well program, Mackenzie Delta, Northwest Territories, Canada. Geological Survey of Canada, Natural Resources Canada, Bulletin 585, pp. 140 (4 sheets), 1 CD-ROM, doi:10.4095/220702 (2005).
42. Dixon, J. (ed.) *Geological Atlas of the Beaufort-Mackenzie Area*. Natural Resources Canada, Ottawa, Ontario, pp. 178, doi:10.4095/207658 (1995).
43. Harrison, J.C. *et al.* *Geological map of the Arctic/ Carte géologique de l'Arctique*; Map 2159A, Geological Survey of Canada, Natural Resources Canada, Ottawa, Ontario, doi: 10.4095/287868 (2011).
44. Norris, D. K. *Geology, Aklavik, District of Mackenzie: A-Series 1517A*, Geological Survey of Canada, Natural Resources Canada, Ottawa, Ontario, doi:10.4095/109706 (1981).
45. Brown, J., Ferrians, Jr. O. J., Heginbottom, J. A. & Melnikov, E. S. (eds) *Circum-Arctic map of permafrost and ground-ice conditions*. Washington, DC: U.S. Geological Survey in Cooperation with the Circum-Pacific Council for Energy and Mineral Resources. Circum-Pacific Map Series CP-45, scale 1:10,000,000, 1 sheet (1997).
46. Latifovic, R., Olthof, I. & Pouliot, D. Land Cover Map of Canada 2005 from MODIS 250m. NRCan, ESS Program: Understanding Canada from Space. Ottawa, Ontario, Canada License: <http://open.canada.ca/en/open-government-licence-canada> (2008).

Acknowledgements

The reanalysis data was provided by the NOAA/OAR/ESRL PSD, Boulder, Colorado, USA from their website at <http://www.esrl.noaa.gov/psd/>. This work was supported by the Helmholtz Association of German Research Centres through a Helmholtz Young Investigators Group grant to T.S. (grant VH-NG-821) and is a contribution to the Helmholtz Climate Initiative REKLIM (Regional Climate Change). The National Ecological Observatory Network is a project solely sponsored by the National Science Foundation and managed under cooperative agreement by NEON, Inc. S.M.'s contribution is based upon work supported by the National Science Foundation under Cooperative Service Agreement EF-1029808. Any opinions, findings, and conclusions or recommendations expressed in this material are those of the author(s) and do not necessarily reflect the views of the National Science Foundation.

Author Contributions

T.S. and J.H. designed the experiment. K.K., T.S., A.S., and J.H. collected the data. J.H. processed the raw data, and K.K. and A.S. further processed and analysed data based on algorithms developed by S.M. and adjusted by S.M., A.S., and K.K. All authors interpreted the results, K.K. wrote the first version of the manuscript, and all authors commented on the manuscript.

Additional Information

Competing Interests: The authors declare that they have no competing interests.

Publisher's note: Springer Nature remains neutral with regard to jurisdictional claims in published maps and institutional affiliations.



Open Access This article is licensed under a Creative Commons Attribution 4.0 International License, which permits use, sharing, adaptation, distribution and reproduction in any medium or format, as long as you give appropriate credit to the original author(s) and the source, provide a link to the Creative Commons license, and indicate if changes were made. The images or other third party material in this article are included in the article's Creative Commons license, unless indicated otherwise in a credit line to the material. If material is not included in the article's Creative Commons license and your intended use is not permitted by statutory regulation or exceeds the permitted use, you will need to obtain permission directly from the copyright holder. To view a copy of this license, visit <http://creativecommons.org/licenses/by/4.0/>.

© The Author(s) 2017